
UNIVERSAL TOPOLOGICAL REGULARITIES OF SYNTACTIC STRUCTURES: DECOUPLING EFFICIENCY FROM OPTIMIZATION

A PREPRINT

 **Fermín Moscoso del Prado Martín**

Department of Language and Communication & Center for Language Studies
Radboud University
Erasmuslaan 1, 6525 NL, Nijmegen, The Netherlands
fermin.moscoso-del-prado@ru.nl

ABSTRACT

Human syntactic structures are usually represented as graphs. Much research has focused on the mapping between such graphs and linguistic sequences, but less attention has been paid to the shapes of the graphs themselves: their topologies. This study investigates how the topologies of syntactic graphs reveal traces of the processes that led to their emergence. I report a *new universal regularity in syntactic structures*: Their topology is communicatively efficient above chance. The pattern holds, without exception, for all 124 languages studied, across linguistic families and modalities (spoken, written, and signed). This pattern can arise from a process *optimizing for communicative efficiency* or, alternatively, by construction, as a by-effect of a *sublinear preferential attachment* process reflecting language production mechanisms known from psycholinguistics. This dual explanation shows how communicative efficiency, per se, does not require optimization. Among the two options, efficiency without optimization offers the better explanation for the new pattern.

Keywords Syntax · Sublinear Preferential Attachment · Communicative Efficiency · Dependency Grammar

Introduction

Human languages map linear sequences of symbols (e.g., sounds, letters, words, etc.) into more elaborate, non-sequential, syntactic structures. Linguists have proposed very diverse formalisms for representing these structures, and for their mapping into the linear sequences. Virtually all linguistic theories –dating as far back as Pāṇini [1] around the 4th century BCE– coincide in using structures that can be modelled as graphs. The meaning of the graph vertices and edges vary depending on the specific theory, ranging from the derivation trees of Generative Grammar paradigms [e.g., 2, 3] to the directed graphs used in Dependency Grammar formalisms [e.g., 4]. An important distinction can be drawn here between the *topology* of the syntactic graphs themselves on the one hand, and their mapping into linguistic sequences –their *linearization*– on the other [4]. Psychologically, the distinction between the topology of the graphs and their linearization is mirrored by separate stages of *function assignment* and *positional processing* during grammatical encoding in language production [5, 6].

Cognitive and functional linguists have long hypothesized that syntactic structures in human languages are particularly efficient for communication [e.g., 7, 8, 9]. In recent years, several studies have provided empirical support for the communicative efficiency of different linguistic aspects, using large-scale data across many languages [10, 11, 12, 13, 14, 15, 16, 17, 18, 19, 20, 21, 22, 23]. Of these studies, those investigating syntactic structures have mainly focused on the emergence of specific properties in the linearization of the structures, taking their actual topologies as a given. These include: the sequential distance between words linked by a syntactic relation [24, 11, 12, 25, 17], the tendency to avoid link crossings within the graphs [11, 25], and how communicative efficiency leads to the emergence of word or morpheme orderings and/or choices that are common across languages [12, 13, 14, 21, 22]. In contrast, the topology itself of the syntactic graphs has received comparatively little empirical attention. In this direction, using insights from Network Science, researchers have noticed that the topology of ‘global’ syntactic graphs (i.e., large graphs

merging the syntactic relations across all utterances in a corpus) exhibit properties of small-world/scale-free networks [26, 27, 28, 29], but such properties do not extend to individual utterances [26].

Many studies interpret the communicative efficiency of linguistic structure as direct evidence that such structures arise through processes that optimize for such efficiency [e.g., 10, 11, 12, 13, 14, 15, 16, 17, 18, 19, 21, 22, 23], rarely even mentioning –let alone comparing with– any alternatives to this optimization. Furthermore, the precise nature of the hypothesized optimization processes remains rather vague. In this respect, most authors point to some –unspecified– selection process operating at either evolutionary, historical, or developmental time scales. In contrast, it has been found that –for some linguistic properties– the communicative efficiency itself may be epiphenomenal, if at all present: What appear to be optimized structures might in fact be just the most likely outcomes irrespective of any optimization [30, 31, 32, 33, 34], or may be side effects of known psycholinguistic mechanisms [34, 35]. It is fairly clear that –as is argued by the studies above– higher communicative efficiency can indeed *result from* optimizing efficiency measures. However, the studies seem to overlook that efficiency might just as well be *the cause* that enabled a basic mechanism to be co-opted for language use, i.e., the mechanism survived because it turned out to result in efficient communication. This is especially relevant for graph structures, as it is known that efficiency in graphs can arise both by optimization and by construction [10, 36, 37].

Measuring the communicative efficiency of a graph’s topology.

In order to benefit from existing corpora [38], I represent syntactic structures using Dependency Grammar [4]. In this formalism, syntactic structures are graphs such as that in Fig. 1A. The graph’s vertices are labelled with the words or morphemes from the sentence, and its edges denote syntactic relations between pairs of words. From an information-theoretical perspective, efficient linguistic structures can be viewed as minimizing an energy function Ω weighting the cost of the structure from the point of view of the speaker and from that of the listener [10],

$$\Omega = \rho C_{\text{listener}} + (1 - \rho) C_{\text{speaker}}, \quad (1)$$

where C_{listener} , C_{speaker} reflect the cost of the structure from the perspective of the listener and of the speaker, respectively, and $0 < \rho < 1$ indexes the relative importance given to each of those costs (i.e., values of $\rho > .5$, prioritize minimizing the cost for the listener, and $\rho < .5$ gives more importance to the cost for the speaker). This model has been successfully applied to account for a variety of aspects of language structure [10, 15, 16, 18, 20, 21, 22]. Applying this model to the topologies of syntactic structures requires defining adequate measures for both C_{listener} and C_{speaker} .

For other aspects of linguistic structure [10, 13, 14, 21, 22] C_{speaker} has been found to be proportional to the Shannon entropy [39] of the specific structure, which is an index of the structure’s heterogeneity and unpredictability. The corresponding measure of entropy for graphs is the entropy of the degree distribution [37], and more specifically for directed trees, the *entropy of the out-degree distribution*. In a dependency tree with N vertices, let k be the number of edges that leave a vertex (i.e., the vertex’s out-degree). One can define a probability distribution $p(k)$ over the values of k in a dependency tree (see Fig. 1C). The entropy of the out-degree distribution is the Shannon entropy over $p(k)$, which is then a measure of the cost of producing the topology of the associated syntactic structure,

$$h_{\text{deg}} = - \sum_{k=0}^{N-1} p(k) \log_2 p(k) \propto C_{\text{speaker}}. \quad (2)$$

From the listener’s standpoint, the cost should be driven by the difficulty of accurately reconstructing the network’s topology from the linear linguistic message. It has been found that star trees are optimal in this respect [10, 37]. More generally, one can expect that such difficulty should be inversely related to the structure’s overall degree of *coherence*: How closely related are the words/concepts expressed by the network? For graphs, this is indexed by their longest or average path lengths, which are minimal for star trees. Furthermore, the communication channel is noisy. Minimizing the effect that transmission errors might have on the reconstructed structure is of crucial importance for the listener. The impact of such errors on graph topologies is measured by the *network’s robustness*. From the undirected skeleton of the dependency structure, that is, the pure topology of the dependency tree, not considering the edge directions (see Fig. 1D), one can define a $N \times N$ binary adjacency matrix A , whose elements $a_{i,j}$ are set to one if vertices i and j are connected (in either direction), and to zero otherwise (see Fig. 1E). The *Kolmogorov-Sinai entropy* of the graph [40] is then defined as

$$h_{\text{ks}} = \log_2 \lambda, \quad (3)$$

where λ denotes A ’s largest positive eigenvalue (i.e., its spectral radius). This measure satisfies the three desiderata above: It is maximal for star graphs, it is negatively correlated with path lengths, and it is a good index of the graph’s robustness [40]. Therefore, a good choice for the listener’s cost function is $C_{\text{listener}} \propto -h_{\text{ks}}$.

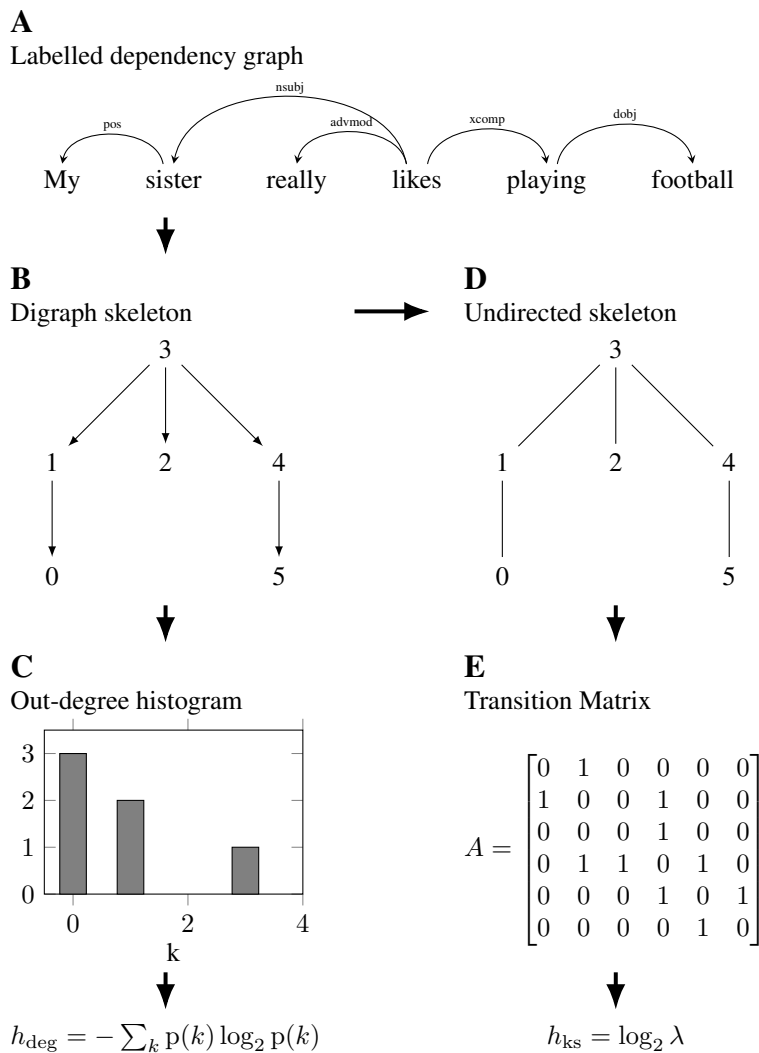


Figure 1: Schema of the computation of the cost measures for each dependency graph. (A) Dependency graph for an English sentence. (B) Digraph skeleton of the dependency graph. (C) Histogram of the out-degrees of the digraph’s nodes, from which the out-degree entropy (h_{deg}) is computed as the Shannon entropy of the relative histogram. (D) Undirected skeleton of the digraph. (E) Transition matrix (A) of the undirected skeleton. The largest positive eigenvalue of A –its spectral radius (λ)– is used for computing the Kolmogorov-Sinai entropy (h_{ks}) of the graph.

Universality of efficiency distributions across languages.

Each yellow dot in Fig. 2 plots the mean normalized values of h_{deg} and h_{ks} for sentences in one of 124 languages, taken from the dependency-annotated corpora of the *Universal Dependencies Project* [38]. As a baseline, for each of language, the purple dots plot the average values of the two measures for uniformly sampled random dependency trees matched in number of vertices to the actual sentences from the corpora. It is clear from the graph that the actual dependency structures found in languages are markedly different from those one would expect by chance. These differences are consistent across languages, reflecting a substantially increased value of H_{ks} with respect to chance (paired $t[123] = 31.2495$, $p < .0001$) holding for every single language studied. This increase is paired with a slight decrease in the average values of H_{deg} (paired $t[123] = -3.8435$, $p = .0002$), which holds for the majority (60%) of languages. Put simply, real dependency structures have a substantially lower average comprehension costs than random ones, which seems to be a universal property, most often paired with a slight decrease in production costs. Most strikingly, the individual dependency graphs (i.e., not just the averages) are sufficiently distinct from chance that they can be correctly classified as real or random syntactic structures with 79% accuracy by a simple logistic classifier

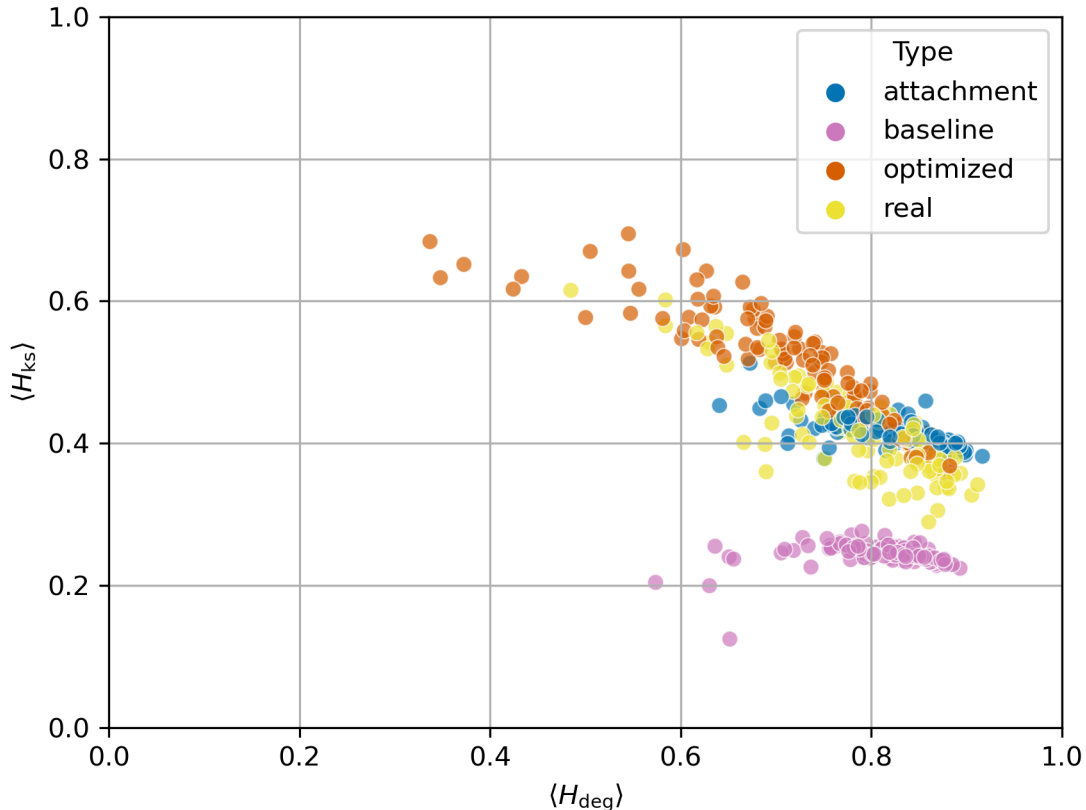


Figure 2: By-language mean values of the normalized (see Materials and Methods) cost measures. Each dot plots a language’s mean values, and its color denotes the type of graphs considered: *yellow*, mean values for real dependency graphs in the corpus, *purple*, mean values for uniformly sampled (matched in sentence length to the real sentences) baseline, *red*, mean values for graphs resulting from applying the optimization algorithm to the baseline graphs, and *blue*, mean values for graphs randomly sampled using a sublinear preferential attachment process (matched in sentence length to the real sentences).

using just their h_{ks} , and h_{deg} values. This accuracy goes up to 85% when one considers only sentences with at least ten words (for which there is much more variability in the values of the cost measures). The increased efficiencies of the graph topologies suggests that, across languages, the dependency structures of sentences could be the result of the joint optimization of Eq. 1.

Efficiency by optimization.

Using the two cost measures defined above, we can rewrite the minimization of Ω of Eq. 1 as the maximization of Λ ,

$$\Lambda = \rho h_{ks} - (1 - \rho) h_{deg} + \varepsilon, \quad (4)$$

where ε denotes normal white noise that limits the possible optimization. The incomplete optimization induced by the noise term reflects that speakers do not have complete freedom over the choice of syntactic structures they use at a given point: On the one hand, some concepts will require very specific topologies for expressing them, with little choice for the speaker. On the other hand, the non-stationary nature of human discourse and dialogue entails that the syntactic structures of previously produced or encountered utterances constrain the choice of possible syntactic structures speakers will use at any given point [41, 42]. Partial optimization is also necessary from a mathematical standpoint: Full, noiseless, optimization of Eq. 1 is known to result in scale-free graphs, with power-law tailed degree distributions [37]. However, individual dependency trees are not fully scale-free, rather showing degree distributions with stretched exponential tails [26].

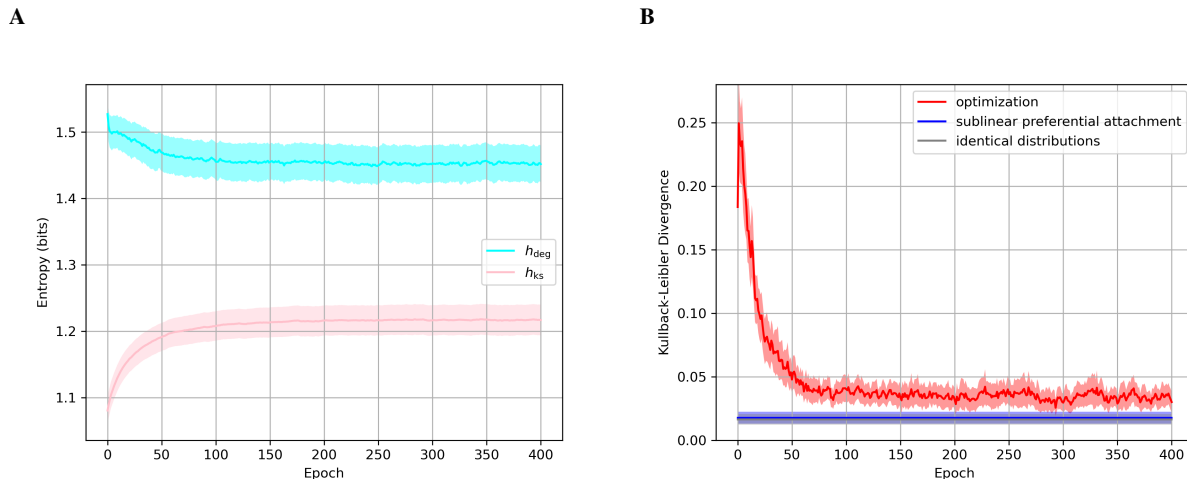


Figure 3: Convergence of algorithms. **(A)** Convergence of the mean values of h_{deg} (light blue) and h_{ks} (pink) through the generations (epochs) of the genetic optimization algorithm. Shaded areas denote 95% C.I. of the mean. **(B)** Estimated Kullback-Leibler divergences (KLDs) between the distribution of the measures for the real graphs in a language, and the graphs generated by optimization (red) and by sublinear preferential attachment (blue). The grey line denotes a ‘zero’ baseline, the KLDs between two subsamples of the real distribution. Shaded areas denote 95% C.I. of the mean.

I applied a genetic algorithm maximizing Λ starting from uniformly sampled random dependency trees (each matched in number of vertices to a sentence in a language). Fig. 3A shows that the values of both cost measures rapidly converge. The optimization consists of a small, but significant, reduction in the production cost (h_{deg}), coupled with a larger reduction in the comprehension cost ($-h_{ks}$). As was predicted, the joint distribution of the cost measures of the gradually optimized graphs rapidly converges on the distribution of the actual cost values for the individual sentences in each language, both distributions being practically undistinguishable at the point of convergence (see Fig. 3B). The resulting –partially-optimized– graphs have per-language mean costs (red dots in Fig. 2) that strongly overlap with those observed in the real sentences (yellow dots in Fig. 2). The algorithm just maximizes the communicative efficiency Λ , naturally resulting in distributions approaching those of actual languages. Note, however, that this optimization is extremely sensitive, with only a precise combination of the model’s parameters (giving more importance to comprehension than to production costs) approximating real language distributions (see convergence analysis in the Materials and Methods section).

Efficiency by construction: Sublinear preferential attachment.

From the perspective of psycholinguistics, grammatical encoding for language production is known to be an incremental cascaded process [5]. Substantial experimental evidence [6] shows that the syntactic structure of an utterance is assembled piecewise, in what is referred to as the *function assignment* process. Rather than assembling the whole structure at once, words become gradually available as the output from the *lexical selection* process, and they are integrated into the syntactic graph as they arrive. Such a process is therefore a rich-get-richer process, that one would expect to result in the higher than random values of h_{ks} that were reported above. Consistently, the types of graphs that arise from the optimization of energy functions such as Ω , can alternatively be understood as being efficient *by construction*, without any actual optimization intervening [37]. In particular, the scale-free networks resulting from optimizing Ω also arise as a result of a preferential attachment process [36]. In such model, a graph is constructed incrementally, adding one vertex at a time, which attaches to one of the vertices already in the network with probability proportional to the number of other vertices that are already attached to it (i.e., proportional to the existing vertex’s degree, $p_{attach} \propto k$). In the same way that a noise term serves to prevent full optimization of individual syntactic graphs, one can obtain a not fully optimal version of the preferential attachment graph by making the probability of attaching to an existing vertex proportional to a power $\alpha \geq 0$ of the vertex’s degree (i.e., $p_{attach} \propto k^\alpha$). When $\alpha < 1$ this is referred to as *sublinear preferential attachment* model [43], and its effects are similar to the partial optimization described earlier, resulting also in the stretched exponential tailed degree distributions that characterize individual dependency graphs.

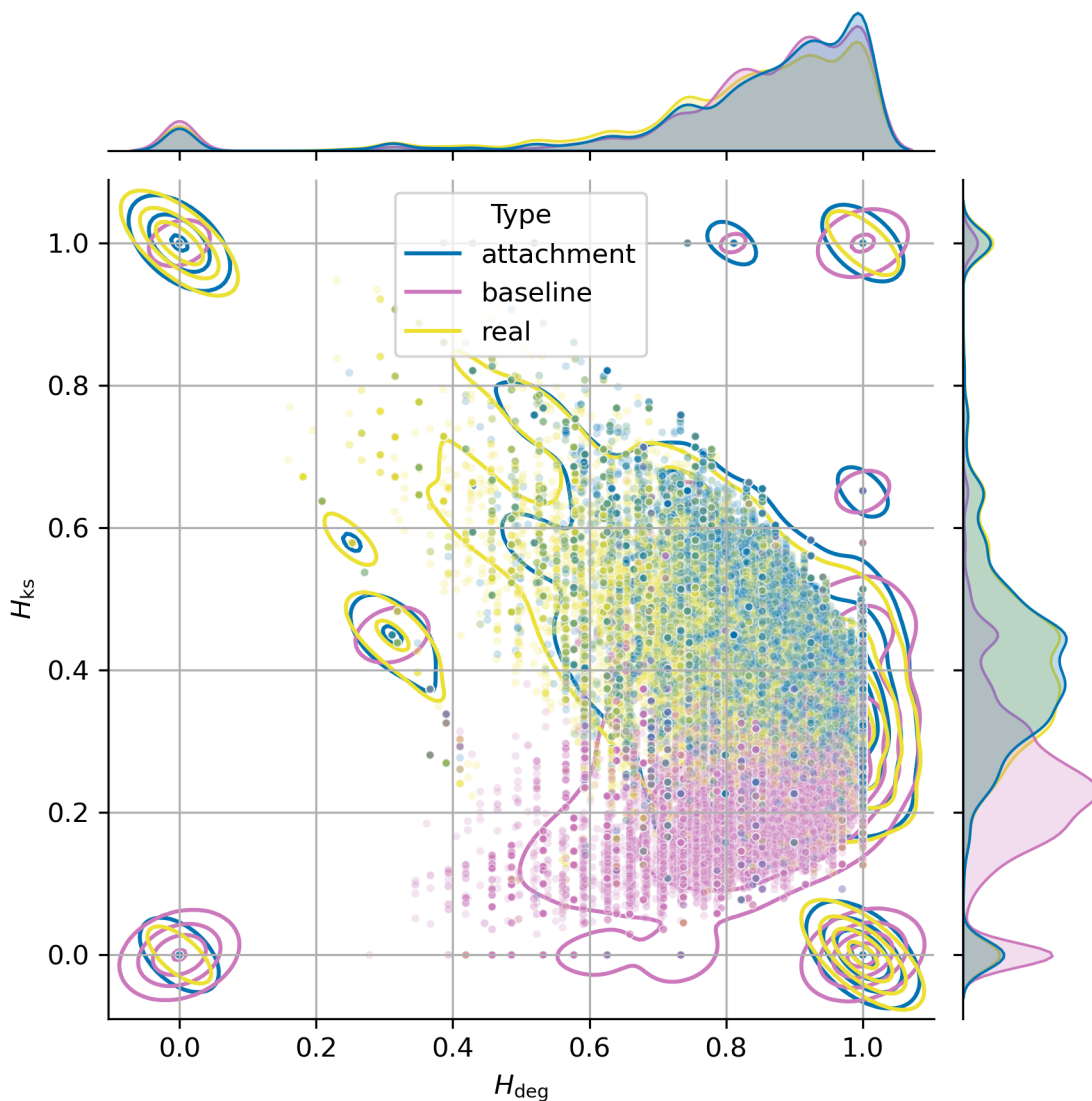


Figure 4: Values of the normalized (see Materials and Methods) cost measures for the individual graphs. Each dot plots one graph, and its color denotes the type of graph considered: *yellow*, real dependency graphs in the corpus, *purple*, uniformly sampled (matched for sentence length to the real sentences) baseline, and *blue*, graphs randomly sampled using a sublinear preferential attachment process (matched in sentence length to the real sentences). The contours plot kernel density estimates in each condition, and the distributions on the margin are kernel density estimates for the marginal distributions.

The blue dots in Fig. 2 plot the mean values of the cost measures for random dependency graphs generated according to a sublinear preferential attachment model matched to the sentences in each of the languages. As predicted, they indeed model very well the distribution observed for the real sentences. This is remarkable as the modelling relies on one single parameter α , that is not “fitted”, but rather assigned a value according to principled considerations based on the number of vertices in the graphs and their maximum degrees [43]. Even more remarkably, the distribution of individual random graphs generated by sublinear preferential attachment is virtually identical to that exhibited by the dependency graphs of actual sentences: The estimated Kullback-Leibler divergence between both distributions is very close to the estimated divergence between identical distributions (see Fig. 3B). This is visible in the strikingly alike marginal and joint distributions of the simulated and real sentences (see Fig. 4). In contrast with the uniform random graphs, a logistic classifier is hardly able to tell the sublinear preferential attachment random graphs apart from the real dependency graphs (55% accuracy; 58% for sentences with ten or more elements). Furthermore, this model is

extremely robust; almost all possible values of its single parameter lead to close approximations of the real distributions, as long as the parameter value indeed corresponds to a sublinear attachment (see stability analysis in the Materials and Methods section).

Discussion.

This study demonstrates how the topologies of individual human syntactic structures allow –across languages and modalities– more efficient communication than what one would expect by chance: Real dependency graphs have a substantially increased noise robustness (h_{ks}), and a slightly reduced heterogeneity (h_{deg}). In other words, real dependency graphs are more “starry” than chance would predict, and “starry” graphs are most efficient for communication [37]. The regularities previously found for global syntactic graphs [26, 27, 28, 29] are therefore paralleled with similar regularities at the individual sentence level.

The new property can be accounted for by two contrasting models: One using explicit noisy optimization of the efficiency measures, and another in which the efficiencies are side effects of a known incremental mechanism for producing syntactic structures [5, 6]. In terms of accounting for the corpus data, both models perform remarkably well [44]. However, one should choose the preferential attachment process over the optimization for several reasons: Statistically speaking, on the one hand the optimization method requires very precisely adjusting two free parameters (the weighting factor and the noise intensity). On the other hand, the preferential attachment model requires just a single parameter (the sublinear exponent), whose value is extremely robust. The second model is therefore more parsimonious than the first and, on equal best performance, it should be preferred [e.g., a Bayes’ Factor would pick the second model over the first one by a wide margin; 45]. Furthermore, arguing that communicative efficiency is the result of evolutionary, historical, or developmental optimization processes comes with a burden of proof: It would require a detailed outline of how such processes take place, together with additional evidence for their presence (e.g., lower communicative efficiencies at earlier evolutionary, historical, or developmental stages). The description of such processes, as well as any evidence for their presence, are conspicuously absent from the literature. In our case, efficiency by construction assumes only the incrementality of grammatical encoding in language production [5], for which ample experimental evidence is available [6]. These results caution against blindly accepting a causal link between communicative efficiency and the presence of optimization processes, unless alternative explanations and additional evidence are considered. Claims for efficiency by optimization could be revisited to investigate whether they could also be accounted for with efficiency by construction.

From the above one should conclude that the increased efficiency of dependency graph topologies is –borrowing Gould and Lewontin’s metaphor– a “spandrel” [46], which emerges from the way speakers build up their syntactic structures. Yet, even without optimization, it remains relevant that human syntactic structures exhibit above-chance communicative efficiency. One should expect human language as a whole [but not necessarily all of its aspects; 33, 34, 35] to be efficient –or rather not inefficient– for communication, least the evolutionary process might have selected against it [e.g., 7, 8, 9]. Indeed, it was *assuming communicative efficiency* in the first place that led to finding the regularities reported here.

Linguists and psycholinguists consistently find that speakers prioritize minimizing their own costs over easing those of the listeners when building syntactic structures [47, 48, 49]. These findings contrast with our finding that the efficiency from the listener’s perspective prevails, which is shared with other optimization-based studies [21, 23]. Decoupling efficiency from optimization by considering efficiency by construction reconciles both findings: The mechanism by which the speaker constructs syntactic structures naturally results in structures that are efficient for the listener as well. Efficiency arises from the structures’ growth patterns, as it does in many other structures in nature [50].

Acknowledgments

Code and data are available online [51]. The author is indebted to Prof. Marco Baroni for helpful suggestions on this manuscript. The author declares no competing interests.

References

- [1] E.V.N. Namboodiri. Panini’s conception of “Syntactic Structures”. *Interdisc. J. Linguist.*, 10:1–16, 2017.
- [2] Noam Chomsky. *Syntactic Structures*. Mouton, The Hague/Paris, 1957.
- [3] Noam Chomsky. *The Minimalist Program*. MIT Press, Cambridge, MA, 1995.
- [4] Lucien Tesnière. *Éléments de Syntaxe Structurale*. Klincksieck, Paris, 1959.

- [5] Willem J. M. Levelt. *Speaking: From Intention to Articulation*. Cambridge, MA, MIT Press, 1989.
- [6] J. Kathryn Bock and Willem J. M. Levelt. Language production: Grammatical encoding. In M. A. Gernsbacher, editor, *Handbook of Psycholinguistics*, pages 945–984. Academic Press, San Diego, 1994.
- [7] Talmy Givón. Markedness in grammar: Distributional, communicative and cognitive correlates of syntactic structure. *Stud. Lang.*, 15:335–370, 1991.
- [8] William Croft and D. Alan Cruse. *Cognitive Linguistics*. Cambridge, UK, Cambridge University Press, 2004.
- [9] John A. Hawkins. *Efficiency and Complexity in Grammars*. Oxford, UK, Oxford University Press, 2004.
- [10] Ramón Ferrer i Cancho and Ricard V. Solé. Least effort and the origins of scaling in human language. *P. Natl. Acad. Sci. USA*, 100:788–701, 2003. doi:10.1073/pnas.0335980100.
- [11] Ramón Ferrer i Cancho. Why do syntactic links not cross? *Europhys. Lett.*, 76:1228–1235, 2006. doi:10.1209/epl/i2006-10406-0.
- [12] Ramón Ferrer i Cancho. Some word order biases from limited brain resources. a mathematical approach. *Adv. Complex Syst.*, 11(3):394–414, 2008. doi:10.1142/S0219525908001702.
- [13] T. Florian Jaeger and Hal J. Tily. On language ‘utility’: Processing complexity and communicative efficiency. *Wiley Interdiscip. Rev. Cogn. Sci.*, 2:323–335, 2011.
- [14] R. Levy and T. Florian Jaeger. Speakers optimize information density through syntactic reduction. In Bernhard Schölkopf, John C. Platt, and Thomas Hoffman, editors, *Advances in Neural Information Processing Systems (NIPS)*, volume 19, pages 849–856. MIT Press, Cambridge, MA, 2011.
- [15] Michael C. Frank and Noah D. Goodman. Predicting pragmatic reasoning in language games. *Science*, 336:998, 2012. doi:10.1126/science.1218633.
- [16] Charles Kemp and Terry Regier. Kinship categories across languages reflect general communicative principles. *Science*, 336:1049–1054, 2012. doi:10.1126/science.121881.
- [17] Richard Futrell, Kyle Mahowald, and Edward Gibson. Large-scale evidence of dependency length minimization in 37 languages. *P. Natl. Acad. Sci. USA*, 112(33):10336–10341, 2015. doi:10.1073/pnas.1502134112.
- [18] Noga Zaslavsky, Charles Kemp, Terry Regier, and Naftali Tishby. Efficient compression in color naming and its evolution. *P. Natl. Acad. Sci. USA*, 115:7937–7942, 2018. doi:10.1073/pnas.1800521115.
- [19] Christophe Coupé, Yoon Mi Oh, Dan Dediu, and François Pellegrino. Different languages, similar encoding efficiency: Comparable information rates across the human communicative niche. *Sci. Adv.*, 5(9):eaaw2594, 2019. doi:10.1126/sciadv.aaw2594. URL <https://www.science.org/doi/abs/10.1126/sciadv.aaw2594>.
- [20] Iván G. Torre, Bartolo Luque, Lucas Lacasa, Christopher T. Kello, and Antoni Hernández-Fernández. On the physical origin of linguistic laws and lognormality in speech. *Royal Soc. Open Sci.*, 6:191023, 2019. doi:10.1098/rsos.191023.
- [21] Michael Hahn, Dan Jurafsky, and Richard Futrell. Universals of word order reflect optimization of grammars for efficient communication. *P. Natl. Acad. Sci. USA*, 117(5):2347–2353, 2020. doi:10.1073/pnas.1910923117.
- [22] Michael Hahn, Judith Degen, and Richard Futrell. Modeling word and morpheme order in natural language as an efficient trade-off of memory and surprisal. *Psychol. Rev.*, 128(4):726–756, 2021. doi:10.1037/rev0000269.
- [23] Sean Trott and Benjamin Bergen. Languages are efficient but, for whom? *Cognition*, 225:105094, 2022.
- [24] Ramón Ferrer i Cancho. Euclidean distance between syntactically linked words. *Phys. Rev. E*, 70:056135, 2004. doi:10.1103/PhysRevE.70.056135.
- [25] Ramón Ferrer i Cancho. Hubiness, length and crossings and their relationships in dependency trees. *Glottometrics*, 25:1–21, 2013.
- [26] Ramón Ferrer i Cancho, Ricard V. Solé, and Reinhard Köhler. Patterns in syntactic dependency networks. *Phys. Rev. E*, 69:051915, 2004. doi:10.1103/PhysRevE.69.051915.
- [27] Haitao Liu. The complexity of Chinese syntactic dependency networks. *Physica A*, 387:3048–3058, 2008. doi:10.1016/j.physa.2008.01.069.
- [28] Bernat Corominas-Murtra, Sergi Valverde, and Ricard V. Solé. The ontogeny of scale-free syntax networks: Phase transitions in early language acquisition. *Adv. Complex Syst.*, 12(3):371–392, 2009. doi:10.1142/S0219525909002192.
- [29] Bernat Corominas-Murtra, Martí Sánchez Fibla, Sergi Valverde, and Ricard V. Solé. Chromatic transitions in the emergence of syntax networks. *Royal Soc. Open Sci.*, 5(12):181286, 2018. doi:10.1098/rsos.181286.

- [30] Benoît B. Mandelbrot. An information theory of the statistical structure of language. In W. Jackson, editor, *Communication Theory*, pages 503–512. Academic Press, New York, NY, 1953.
- [31] George A. Miller. Some effects of intermittent silence. *Am. J. Psychol.*, 70(2):311–314, 1957.
- [32] Ramón Ferrer i Cancho and Fermín Moscoso del Prado. Information content versus word length in random typing. *J. Stat. Mech.*, page L12002, 2011.
- [33] Fermín Moscoso del Prado. The missing baselines in arguments for the optimal efficiency of languages. In M. Knauff, M. Pauen, N. Sebanz, and I. Wachsmuth, editors, *Proceedings of the 35th Annual Conference of the Cognitive Science Society*, pages 1032–1037. Cognitive Science Society, Austin, TX, 2013.
- [34] Tiago Pimentel, Irene Nikkarinen, Kyle Mahowald, Ryan Cotterell, and Damián Blasi. How (non-)optimal is the lexicon? In *Proceedings of the 2021 Conference of the North American Chapter of the Association for Computational Linguistics: Human Language Technologies, Volume 1 (Long and Short Papers)*, Virtual, June 2021. Association for Computational Linguistics.
- [35] Spencer Caplan, Jordan Kodner, and Charles Yang. Miller’s monkey updated: Communicative efficiency and the statistics of words in natural language. *Cognition*, 205:104466, 2020.
- [36] Albert-László Barabási and Réka Albert. Emergence of scaling in random networks. *Science*, 286:509–512, 1999. doi:10.1126/science.286.5439.509.
- [37] Ramón Ferrer i Cancho and Ricard V. Solé. Optimization in complex networks. In *Lecture Notes in Physics*, volume 625, pages 114–126. Springer, Berlin, 2003. doi:10.1007/978-3-540-44943-0_7.
- [38] Marie-Catherine de Marneffe, Christopher D. Manning, Joakim Nivre, and Daniel Zeman. Universal Dependencies. *Comput. Linguist.*, 47(2):255–308, 2021. doi:10.1162/coli_a_00402.
- [39] Claude E. Shannon. A mathematical theory of communication. *Bell Systems Tech. J.*, 27:623–656, 1948.
- [40] Lloyd Demetrius and Thomas Manke. Robustness and network evolution — an entropic principle. *Physica A*, 346:682–696, 2005. doi:10.1016/j.physa.2004.07.011.
- [41] J. Kathryn Bock. Syntactic persistence in language production. *Cogn. Psychol.*, 18:355–387, 1986. doi:10.1016/0010-0285(86)90004-6.
- [42] Holly Branigan and Martin Pickering. Structural priming and the representation of language. *Behav. Brain Sci.*, 40:E313, 2017. doi:10.1017/S0140525X17001212.
- [43] Pavel L. Krapivsky, Sidney Redner, and François Leyvraz. Connectivity of growing random networks. *Phys. Rev. Lett.*, 85(21):4629–4632, 2000. doi:doi.org/10.1103/PhysRevLett.85.4629.
- [44] Note1. Although the sublinear preferential attachment method slightly outperforms the optimization algorithm (see Fig. 3B), it is clear that a more exhaustive fine-tuning of the optimization parameters would lead to equally good ‘fitting’ of the distribution by both methods. Note, however, that the sensitivity of the optimization algorithm to its parameter values contrasts with the robustness of the single parameter of the sublinear preferential attachment model.
- [45] Robert E. Kass and Adrian E. Raftery. Bayes factors. *J. Am. Stat. Assoc.*, 90(430):773–795, 1995. doi:10.1080/01621459.1995.10476572.
- [46] Stephen J. Gould and Richard C. Lewontin. The spandrels of San Marco and the panglossian paradigm: A critique of the adaptationist programme. *Proc. R. Soc. B*, 205(1161):581–598, 1979. doi:10.1098/rspb.1979.0086.
- [47] Steven C. Levinson. *Presumptive Meanings: The Theory of Generalized Conversational Implicature*. MIT Press, Cambridge, MA, 2000.
- [48] Victor S. Ferreira. Ambiguity, accessibility, and a division of labor for communicative success. *Psychol. Learn. Motiv.*, 49:209–246, 2008. doi:10.1016/S0079-7421(08)00006-6.
- [49] Maryellen C. MacDonald. How language production shapes language form and comprehension. *Frontiers Psychol.*, 4, 2013. ISSN 1664-1078. doi:10.3389/fpsyg.2013.00226. URL <https://www.frontiersin.org/articles/10.3389/fpsyg.2013.00226>.
- [50] D’Arcy Wenworth Thompson. *On Growth and Form*. Cambridge University Press, Cambridge, UK, 1917.
- [51] Note2. <https://doi.org/10.5281/zenodo.7566835> .

Supplementary Materials for:

Universal Topological Regularities of Syntactic Structures: Decoupling Efficiency from Optimization

Fermín Moscoso del Prado Martín

Correspondence to: fermin.moscoso-del-prado@ru.nl

This PDF file includes:

Materials and Methods

References (52-60)

Figs. S1 to S3

Table S1

Algorithms S1 and S2

arXiv:2302.00129v1 [cs.CL] 31 Jan 2023

Materials and Methods

Corpora and preprocessing

I used the treebank corpora in the *Universal Dependencies Project v2.11* (38, 52). For each of the available languages, I concatenated all the treebanks listed for that language. As the cost measures do not have any variability for $N < 4$ (i.e., all trees with fewer than four vertices are simultaneously line and star graphs), I selected only dependency graphs with at least four vertices. In addition, to limit processing costs, I discarded any dependency trees with more than 50 vertices (this amounts to excluding fewer than 2% of the available sentences for any language). I deleted any punctuation vertices, and I considered only the basic vertices in the tree, skipping all “range” vertices (e.g., “3–4” in CONLL format). I deleted all relation labels, and the vertex labels were replaced with plain numbers. I ensured that the resulting dependency structures were actual trees, discarding any that were not. For each language for which there were at least 50 sentences left in the corpus after applying the filters above, I randomly sampled (without replacement) a maximum of 1,000 sentences, if so many were available, or took all available sentences otherwise. By this method, I obtained samples for 124 languages with at least 50 sentences. For each of the dependency graphs, I computed the cost measures h_{deg} and h_{ks} using Eq. 2 and Eq. 3, respectively. Details of the languages considered, their sample sizes and estimated measures are provided in Table S1 (53).

Although sample sizes ranging from just 50 to 1,000 sentences might seem small, the by-language means of the key measures h_{ks} and h_{deg} are unbiased and converge rapidly according to the Central Limit Theorem, with convergence speed proportional to the square root of the sample size. With 50 values, all means were indeed stable (see standard errors in Table S1), enabling the consideration of a large sample of languages.

Normalization of entropy measures

The values of both entropy measures h_{ks} and h_{deg} are dependent of the number of vertices (N) in a tree. To facilitate comparison of the entropies for sentences of different lengths, I used length-normalized versions of both entropies. Note that this normalization was used only for comparisons and plots, all computations were done on the untransformed measures in their natural scales. For a tree of N vertices (i.e., a sentence of N words) I normalized the measures to their relative values in the $[0, 1]$ interval,

$$H_{\text{ks}} = \frac{h_{\text{ks}} - \min_N h_{\text{ks}}}{\max_N h_{\text{ks}} - \min_N h_{\text{ks}}}, \quad H_{\text{deg}} = \frac{h_{\text{deg}} - \min_N h_{\text{deg}}}{\max_N h_{\text{deg}} - \min_N h_{\text{deg}}}. \quad (\text{S1})$$

The extreme values for h_{ks} are quite straightforward. On the one hand, h_{ks} always takes its maximum for a star graph. The eigenvalues of its adjacency matrix A are the roots of its characteristic polynomial,

$$\det(A - \lambda \cdot I) = \begin{vmatrix} -\lambda & 1 & 1 & \cdots & 1 \\ 1 & -\lambda & 0 & \cdots & 0 \\ 1 & 0 & \ddots & \ddots & \vdots \\ \vdots & \vdots & \ddots & \ddots & 0 \\ 1 & 0 & \cdots & 0 & -\lambda \end{vmatrix} = 0.$$

This determinant can be decomposed recursively into minors, to find that –for any N – it has its maximum positive root at $\sqrt{N-1}$. Therefore:

$$\max_N h_{\text{ks}} = \frac{1}{2} \log_2(N-1).$$

Similarly, h_{ks} takes its minimum value for line graphs. A line graph of N vertices has a characteristic polynomial,

$$\det(A - \lambda \cdot I) = \begin{vmatrix} -\lambda & 1 & 0 & \cdots & 0 \\ 1 & -\lambda & 1 & \cdots & 0 \\ 0 & 1 & \ddots & \ddots & \vdots \\ \vdots & \vdots & \ddots & \ddots & 1 \\ 0 & 0 & \cdots & 1 & -\lambda \end{vmatrix} = 0.$$

It is difficult to find a general closed form of this polynomial's roots for all values of N . However, they are easily computed for a specific N , so one just finds the largest positive eigenvalue λ and then applies Eq. 3. One can note, however, that the value of $\min_N h_{ks}$ converges on 1.0 from below for large N .

With respect to h_{deg} , its minimum value is taken for line graphs and star graphs, both of which have all vertices but one having the same degree, therefore,

$$\min_N h_{deg} = \log_2 N - \frac{N-1}{N} \log_2(N-1),$$

which converges on zero from above for large N . On the other hand, the value of $\max_N h_{deg}$ is difficult to compute in closed form, as it is related to the integer sum partitions of $N-1$. It can be computed exactly using Algorithm S1. As this algorithm can be slow for large values of N , I precomputed the values of the four extrema for N up to 50 before running the remaining simulations. An interesting observation is that $\max_N h_{deg}$ appears to converge from below on exactly two bits. I have observed this empirically, but I have not been able to come up with a demonstration, therefore I leave this as a conjecture.

Uniform sampling of directed trees

There are exactly N^{N-2} different trees that can be constructed with N labelled vertices (54). Each such tree can be uniquely identified by a *Prüfer Sequence* (55); a unique sequence of length $N-2$ on the vertex labels 0 to $N-1$. In turn, each labelled tree corresponds to N different rooted trees, each arising from choosing a different vertex as the tree's root. Each rooted tree corresponds to a single directed tree (i.e., choosing the root determines the directionality of all edges). We can therefore create an what I call an *extended Prüfer Sequence* by adding a number identifying the root to the standard Prüfer Sequence. Uniform sampling of directed trees then becomes a straightforward multinomial sampling of Extended Prüfer Sequences of length $N-1$. Using this method, I sampled a random tree with the number of vertices matched to the number of vertices of each dependency tree selected from the corpora. As above, the cost measures for the uniformly sampled graphs were computed using Eqs. 2 and 3.

Optimization algorithm

For optimization of the random trees I used a mutation-only genetic algorithm. The Extended Prüfer Sequences described above constitute the genetic representation of the trees (similar to previous approaches; e.g., 56, 57; but see also 58). Mutation happens by randomly changing a single element of the extended Prüfer Sequence, obtaining what I term an *extended Prüfer Neighbor*. In every generation of trees, all trees were randomly mutated, and selection would take place choosing between the original and the mutated tree according to their estimated fitness levels (i.e., the values of Λ): If the original tree had cost values h_{ks} and h_{deg} , and the

mutated tree had values h'_{ks} and h'_{deg} , the mutated tree would be selected over the original if the discrete gradient ($\Delta\Lambda$) is greater than zero,

$$\Delta\Lambda = \Lambda' - \Lambda = \rho(h'_{ks} - h_{ks}) - (1 - \rho)(h'_{deg} - h_{deg}) + \varepsilon > 0,$$

and the original tree was kept otherwise. The random noise term $\varepsilon \sim \mathcal{N}(0, \sigma)$ governs the stochastic part of the selection process. As discussed in the main text, it has an optimization-halting effect: When the discrete gradients become smaller than the average noise, the noise halts the optimization.

The genetic algorithm above was applied for 400 epochs (i.e., generations) on a sample of 100 of the random trees generated as baselines for each language (or all trees for those languages for which fewer than 100 trees were available). The optimization weight was set to $\rho = .9$, and the noise standard deviation to $\sigma = .075$. These parameter values were chosen by examining the convergence patterns of the algorithm for different values. Fig. S1 plots the evolution of the mean values $\langle H_{deg} \rangle$ and $\langle H_{ks} \rangle$ epoch by epoch. Values of ρ prioritizing the minimization of the production cost (i.e., $\rho < .5$; paths in shades of blue in Fig. S1) are clearly unsuitable, as they end up minimizing just $\langle H_{deg} \rangle$, completely ignoring $\langle H_{ks} \rangle$, towards a local minimum representing line graphs, at position (0,0) in the graph. In turn, when it favours minimizing the comprehension cost or gives equal importance to both costs (i.e., $\rho \geq .5$; paths in shades of yellow and red in Fig. S1), the algorithm has a tendency to converge on the true global minimum, star graphs, which are optimal both in terms of production and comprehension and correspond to position (0,1) in the graph. The noise term σ limits the possible optimization (i.e., not all ideas can be expressed by a star graph), stopping somewhere along the paths plotted in the figure, and hovering around it from then on. Higher values of σ entail an earlier stopping point. Note that only values of ρ closely around $\rho = .9$ result in optimization paths going through the target value (denoted by the star in the plot). Within this path, we find that values of sigma between .07 and .1 result in the optimization halting roughly around the values found in real languages (see the green path in the graph, corresponding to the parameter values we actually employed). Importantly, although optimizing only the efficiency from the comprehender’s perspective (i.e., ρ), ignoring the cost for the listener, is also bound to converge on the same maximum (star graphs; 37), the optimization path does not go through the target. In other words, although most importance should be given to the comprehension cost, obtaining distributions similar to those of actual language still requires simultaneously minimizing the production costs.

Estimation of Kullback-Leibler Divergences

In order to assess the performance of the optimization algorithms, I consider the distributions of h_{ks} and h_{deg} generated for each of the languages, separately for each of the four conditions (real trees, random trees, optimized trees, preferential attachment trees). For each of the last three conditions, the degree of convergence to the distribution of the real trees is measured by the Kullback-Leibler Divergence (KLD; 59), between the real distribution (p_{real}) and each of the conditions (p_X):

$$D(p_{real} || p_X) = \int_0^\infty \int_0^\infty p_{real}(h_{ks}, h_{deg}) \log \frac{p_{real}(h_{ks}, h_{deg})}{p_X(h_{ks}, h_{deg})} dh_{ks} dh_{deg}.$$

Rather than using numerical approximations (e.g., through nearest neighbors) for estimating KLD, I used a parametric approximation, approximating each distribution by a bivariate Gaussian distribution. For this, I estimated the vector means in each condition for each language,

$$\boldsymbol{\mu}_{language} = (\langle h_{ks} \rangle_{language}, \langle h_{deg} \rangle_{language})^T,$$

and the corresponding 2×2 covariance matrices Σ_{language} , under each condition. The KLD between two bivariate Gaussians (P, Q) with vector means $\boldsymbol{\mu}, \boldsymbol{m}$ and covariance matrices Σ, S , respectively, is calculated using the closed form expression

$$D(P\|Q) = \frac{1}{2} \left(\text{tr}(S^{-1}\Sigma) - 2 + (\boldsymbol{m} - \boldsymbol{\mu})S^{-1}(\boldsymbol{m} - \boldsymbol{\mu}) + \log \frac{\det(S)}{\det(\Sigma)} \right).$$

Even for truly identical distributions, the KLD estimates depend on the sample sizes used for their estimation, and on how well the distributions are modelled by a bivariate Gaussian. In order to provide a ‘zero’ baseline against which to compare the KLD estimates, I used a bootstrap method (60): For each sample of real graphs I computed its KLD to another an equally-sized resampling with replacement from the original sample. Relatedly, whenever comparing distributions with different sample sizes, I downsampled the larger sample to the size of the smaller one prior to computing the KLDs. For instance, see the difference in the values of the red and grey lines between Fig. 3 and Fig. S3. These lines represent the same KLDs in both plots. However, Fig. 3 compares with the optimization results (for which there were fewer values). This required downsampling of these distributions in Fig. 3, but not in Fig. S3.

Sublinear preferential attachment tree sampling

In graphs exhibiting sublinear preferential attachment, the highest degree among their vertices (k_{max}) can be asymptotically approximated (43) as a function of their number of vertices N and their sublinear exponent $0 < \alpha < 1$,

$$k_{\text{max}} \sim (\log N)^{\frac{1}{1-\alpha}}. \quad (\text{S2})$$

One can derive an estimator for α from this approximation:

$$\hat{\alpha} = 1 - \frac{\log \log N}{\log k_{\text{max}}}, \text{ for } N > 1. \quad (\text{S3})$$

I computed the estimator $\hat{\alpha}$ using Eq. S3 for each of the dependency trees sampled from the treebanks. For each language, I estimated its α value as the mean of the $\hat{\alpha}$ values among its sentences $\langle \hat{\alpha} \rangle_{\text{language}}$. Finally, for each dependency tree in each language I sampled a random tree by preferential attachment with the α set to the value of $\langle \hat{\alpha} \rangle_{\text{language}}$ corresponding to that language. The nonlinear preferential attachment trees were sampled using Algorithm S2.

Eq. S2 is valid only when a tree is actually the result of a sublinear preferential attachment process. However, the estimator in Eq. S3 can be computed for any tree, whether or not it actually results from sublinear preferential attachment. The estimator can produce apparently correct values of $\hat{\alpha} < 1$ even for trees that are plainly random, but such estimates would be meaningless (i.e., estimating that $\hat{\alpha} < 1$ does not constitute a valid *statistical test* for sublinear preferential attachment). However it is easy to distinguish estimates arising from sublinear preferential attachment from spurious ones. If a set of trees does indeed result from sublinear preferential attachment, generating a new set of trees using the estimated $\hat{\alpha}$ value will result in a distribution of trees very similar the original one. However, generating new trees using an $\hat{\alpha}$ value estimated from trees not originating in sublinear preferential attachment will result in a substantially altered distribution of trees.

In the current case, the real language graphs exhibited significantly larger estimated exponent values ($\langle \hat{\alpha} \rangle = .4197 \pm .0045$) than did the uniform random graphs ($\langle \hat{\alpha} \rangle = .3041 \pm .0067$). The random graphs generated using the estimated $\hat{\alpha}$ estimates from the real graphs resulted in almost identical distributions (see Fig. 4). In contrast, generating sublinear preferential attachment graphs using the $\hat{\alpha}$ estimates from uniform random graphs resulted in markedly different

distributions (see Fig. S2). Incidentally, notice that the distribution of sublinear attachment graphs regenerated using the $\hat{\alpha}$ values from the uniform random graphs is in fact extremely similar to the actual distribution of real graphs in Fig. 4. This is not accidental. The sublinear preferential attachment process is in fact *extremely robust* in terms of estimates. If, instead of estimating the value of $\hat{\alpha}$ for each language, I had just picked a fixed value for all languages, with the only constraint that it be sublinear (i.e., $\alpha < 1$; left of the dashed line in Fig.S3), the resulting distributions would still mimic those found in actual dependency graphs. As is shown in Fig. S3, any value of α between .25 and .75 provides essentially an equally good model of the real-language dependency graph distribution, and even the values in the intervals $[0, .25)$ and $(.75, 1)$ remain extremely good approximations. Only when one moves into superlinear preferential attachment (43) territory (i.e., $\alpha > 1$; right of the dashed line in Fig.S3) do the distributions truly diverge. Taken together, these findings reinforce the claim that the dependency graphs found in human language do indeed correspond to the result of a sublinear preferential attachment process.

Logistic classifiers

In order to assess the degree to which it is possible to distinguish between individual real and random graphs I trained four (two distinguishing between real and uniform graphs, and two distinguishing between real and sublinear preferential attachment; in each case a model used all available graphs, and the other only graphs with at least ten vertices) binary logistic classifiers on a randomly chosen 90% of the data, and tested it on predicting the remaining 10%. In each case, one model was trained on all sentences, and the other was trained on sentences having at least ten words. The features used for prediction were the normalized entropy measures H_{ks} and H_{deg} .

References

52. The corpora were downloaded from <http://hdl.handle.net/11234/1-4923>.
53. The mean sentence lengths in each language should not be interpreted as typologically meaningful (e.g., as in highly inflected languages resulting in shorter sentences): The registers and modalities from which the corpora originate differ markedly across the languages. It is these factors, rather than meaningful typological differences, that affect most the sentence lengths in our dataset.
54. A. Cailey, *Quart. J. Pure Appl. Math.* **23**, 376 (1889).
55. H. Prüfer, *Arch. Math. Phys.* **27**, 742 (1918).
56. F. N. Abuali, D. A. Schoenefeld, R. L. Wainwright, *Proceedings of the 1994 ACM Symposium on Applied Computing* (1994), p. 242–246.
57. G. Zhou, M. Gen, *Eng. Design Automat.* **3**, 157 (1997).
58. J. Gottlieb, B. A. Julstrom, G. R. Raidl, F. Rothlauf, *Proceedings of the 3rd Annual Conference on Genetic and Evolutionary Computation, GECCO'01* (Morgan Kaufmann Publishers Inc., San Francisco, CA, USA, 2001), p. 343–350.
59. S. Kullback, R. A. Leibler, *Ann. Math. Stat.* **22**, 79 (1951).
60. B. Efron, *Ann. Stat.* **7**, 1 (1979).

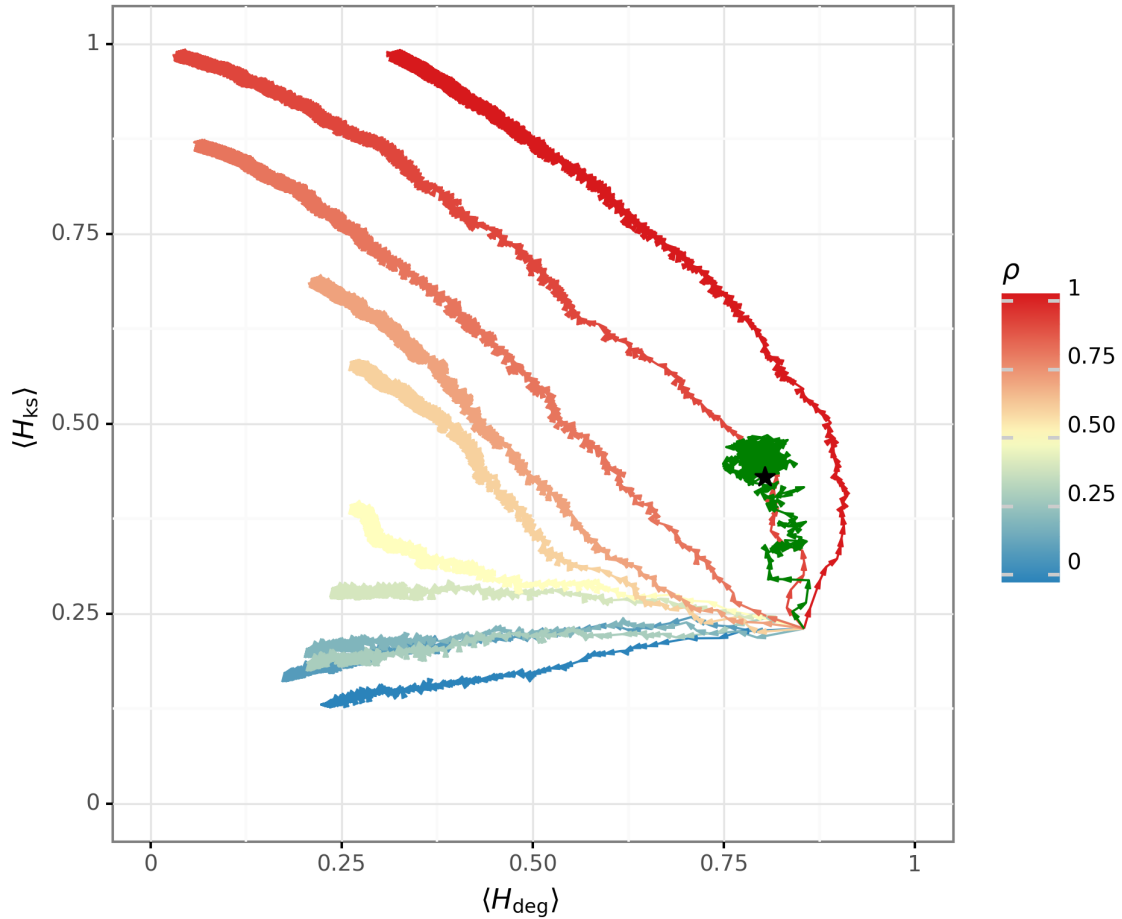


Fig. S1: Sensitivity of the optimization algorithm to variation in the parameters. The paths plot how the mean normalized values of both entropy measures change along the optimization process. All paths start at the average values for the uniform random sampled graphs (matched to the English corpus). The paths ranging in color from blue to red plot different values of ρ , with σ fixed at zero. The green path plots the actual optimization for English in this study, with parameters $\rho = .9$ and $\sigma = .075$. The star denotes the average values for the real English dependency graphs.

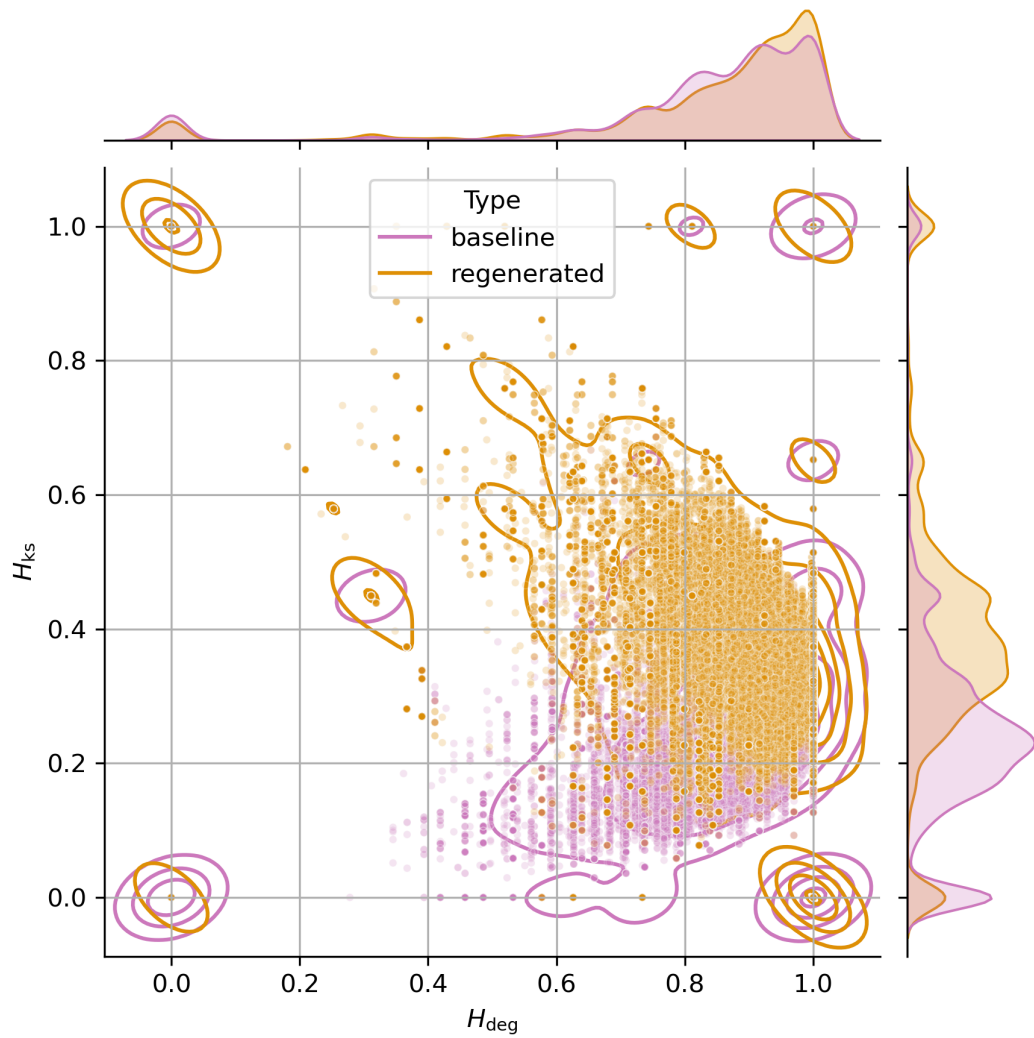


Fig. S2: Normalized entropy values for a distribution (*orange*) generated using the $\hat{\alpha}$ estimates obtained from uniformly sampled graphs (*purple*). The contours plot kernel density estimates in each condition, and the distributions on the margin are kernel density estimates for the marginal distributions. Note the strong similarity between the regenerated distribution and the distribution of sentences in real language depicted in Fig.4

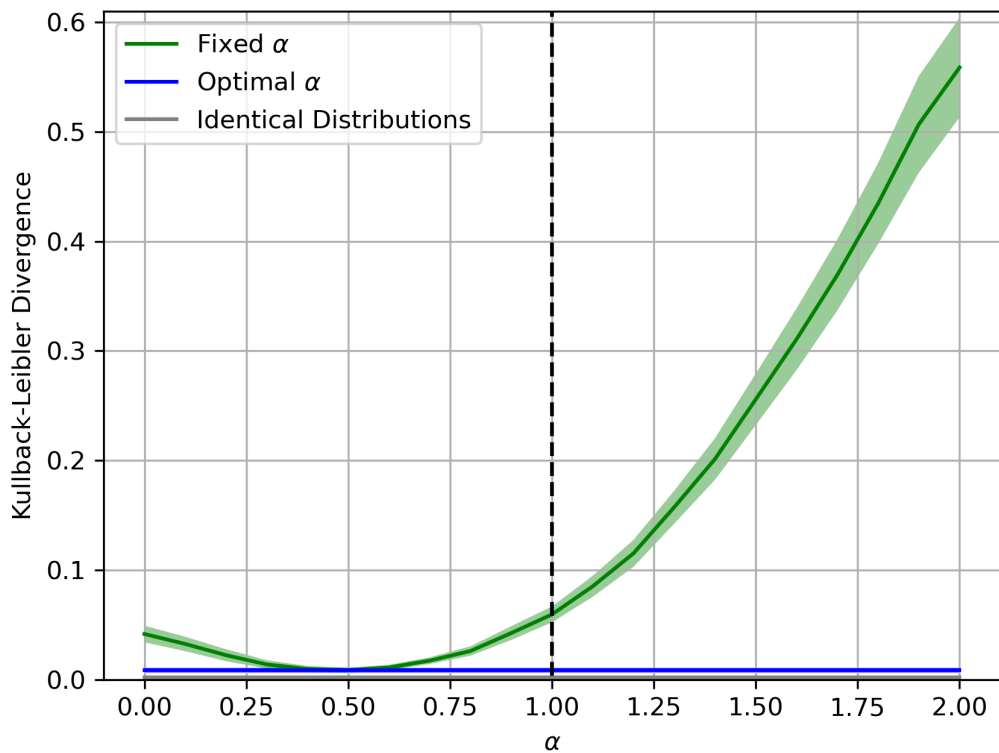


Fig. S3: Estimated Kullback-Leibler divergences between the distribution of the measures for the real graphs in a language, and the graphs generated by sublinear preferential attachment with an arbitrary fixed value of α (*green*), and with the optimal value of α for each language (*blue*). The *grey* line denotes a ‘zero’ baseline. Shaded areas denote 95% C.I. of the mean. The vertical dashed line separates the sublinear zone (left) from the superlinear zone (right).

Table S1: Languages used in the study. Extinct languages, in the sense of not having any remaining native speakers, are marked by †. The mean normalized entropy values $\langle H_{ks} \rangle$ and $\langle H_{deg} \rangle$ are followed by their standard errors.

Language	Family	Group	N. Sents	Mean Sent. Length	$\langle H_{ks} \rangle \pm SE$	$\langle H_{deg} \rangle \pm SE$
Abaza	N.W. Caucasian	Abazgi	86	7.19	.389 ± .033	.796 ± .031
Afrikaans	Indo-European	Germanic	1,000	21.64	.413 ± .003	.813 ± .004
Akkadian†	Afro-Asiatic	Semitic	1,000	12.24	.305 ± .006	.870 ± .006
Akuntsu	Tupian	Tupari	93	5.38	.401 ± .040	.666 ± .042
Albanian	Indo-European	Albanian	60	13.95	.358 ± .013	.894 ± .014
Amharic	Afro-Asiatic	Semitic	1,000	8.66	.541 ± .007	.631 ± .008
Ancient Greek†	Indo-European	Greek	1,000	12.87	.460 ± .006	.776 ± .007
Ancient Hebrew†	Afro-Asiatic	Semitic	1,000	21.38	.387 ± .002	.888 ± .003
Apurinā	Arawakan	Southern	98	5.90	.378 ± .036	.751 ± .037
Arabic	Afro-Asiatic	Semitic	1,000	26.01	.327 ± .004	.905 ± .005
Armenian	Indo-European	Armenian	1,000	15.35	.397 ± .006	.839 ± .006
Bambara	Mande	Western	919	11.85	.441 ± .006	.777 ± .007
Basque	<i>isolate</i>		1,000	11.69	.438 ± .006	.791 ± .007
Beja	Afro-Asiatic	Cushitic	52	13.06	.439 ± .027	.791 ± .034
Belarusian	Indo-European	Slavic	1,000	10.81	.378 ± .007	.826 ± .007
Bhojpuri	Indo-European	Indic	343	16.31	.446 ± .009	.794 ± .010
Breton	Indo-European	Celtic	807	10.77	.465 ± .007	.753 ± .009
Bulgarian	Indo-European	Slavic	1,000	12.45	.413 ± .006	.817 ± .007
Buryat	Mongolic	Central	844	9.60	.353 ± .008	.803 ± .009
Cantonese	Sino-Tibetan	Sinitic	835	12.76	.554 ± .008	.648 ± .011
Catalan	Indo-European	Romance	1,000	25.99	.382 ± .003	.856 ± .004
Cebuano	Austronesian	Central Philippine	150	6.58	.352 ± .023	.809 ± .024
Chinese	Sino-Tibetan	Sinitic	1,000	19.83	.393 ± .004	.873 ± .004
Chukchi	Chukotko-Kamchatkan	Chukotkan	653	6.62	.510 ± .013	.648 ± .015
Classical Chinese†	Sino-Tibetan	Sinitic	1,000	5.86	.346 ± .010	.782 ± .010
Coptic†	Afro-Asiatic	Egyptian	1,000	21.90	.451 ± .003	.810 ± .004
Croatian	Indo-European	Slavic	1,000	19.06	.378 ± .003	.873 ± .004
Czech	Indo-European	Slavic	1,000	15.52	.379 ± .005	.844 ± .006
Danish	Indo-European	Germanic	1,000	16.64	.442 ± .005	.795 ± .007
Dutch	Indo-European	Germanic	1,000	14.51	.436 ± .005	.794 ± .006
Emerillon	Tupian	Maweti-Guarani	132	4.64	.428 ± .036	.696 ± .036
English	Indo-European	Germanic	1,000	16.11	.430 ± .005	.804 ± .006
Erzya	Uralic	Mordvin	1,000	8.66	.416 ± .008	.768 ± .009

Continued on next page

Table S1: (continued)

Language	Family	Group	N. Sents	Mean Sent. Length	$\langle H_{ks} \rangle \pm SE$	$\langle H_{deg} \rangle \pm SE$
Estonian	Uralic	Finnic	1,000	12.40	.447 \pm .006	.767 \pm .008
Faroese	Indo-European	Germanic	1,000	14.64	.472 \pm .006	.764 \pm .007
Finnish	Uralic	Finnic	1,000	10.07	.435 \pm .007	.774 \pm .008
French	Indo-European	Romance	1,000	20.77	.405 \pm .004	.818 \pm .005
Frisian/Dutch	<i>code switching</i>		385	9.58	.564 \pm .010	.637 \pm .013
Galician	Indo-European	Romance	1,000	29.08	.356 \pm .003	.867 \pm .003
German	Indo-European	Germanic	1,000	16.94	.423 \pm .004	.815 \pm .005
Gheg	Indo-European	Albanian	955	15.65	.485 \pm .005	.753 \pm .006
Gothic [†]	Indo-European	Germanic	1,000	11.03	.470 \pm .007	.751 \pm .008
Greek	Indo-European	Greek	1,000	21.79	.375 \pm .003	.846 \pm .004
Guajajára	Tupian	Maweti- Guarani	1,000	7.15	.565 \pm .010	.584 \pm .011
Hebrew	Afro-Asiatic	Semitic	1,000	22.83	.342 \pm .003	.912 \pm .003
Hindi	Indo-European	Indic	1,000	19.86	.428 \pm .003	.847 \pm .004
Hindi/English	<i>code switching</i>		1,000	12.71	.468 \pm .004	.778 \pm .005
Hittite [†]	Indo-European	Anatolian	130	9.95	.481 \pm .020	.733 \pm .024
Hungarian	Uralic	Ugric	1,000	20.04	.382 \pm .004	.881 \pm .004
Icelandic	Indo-European	Germanic	1,000	17.80	.459 \pm .005	.777 \pm .006
Indonesian	Austronesian	Malayo- Sumbawan	1,000	18.22	.355 \pm .004	.887 \pm .004
Irish	Indo-European	Celtic	1,000	20.04	.383 \pm .004	.868 \pm .005
Italian	Indo-European	Romance	1,000	18.48	.411 \pm .004	.799 \pm .006
Japanese	Japonic	Japanese	1,000	17.61	.423 \pm .006	.821 \pm .007
Javanese	Austronesian	Javanese	123	14.31	.364 \pm .012	.869 \pm .012
Kangri	Indo-European	Indic	281	7.77	.513 \pm .014	.695 \pm .017
Karelian	Uralic	Finnic	220	11.38	.422 \pm .012	.808 \pm .014
Karo	Tupian	Ramarama	297	4.85	.615 \pm .023	.485 \pm .025
Kazakh	Turkic	N.W.	958	8.49	.345 \pm .008	.800 \pm .008
K'iche'	Mayan	Greater Quichean	1,000	6.69	.321 \pm .009	.819 \pm .009
Komi-Permyak	Uralic	Permian	86	8.10	.438 \pm .029	.721 \pm .034
Komi-Zyrian	Uralic	Permian	787	10.24	.454 \pm .008	.763 \pm .009
Korean	<i>isolate</i>		1,000	11.69	.330 \pm .006	.848 \pm .006
Kurmanji	Indo-European	Iranian	743	12.05	.429 \pm .005	.824 \pm .006
Latin [†]	Indo-European	Italic	1,000	14.10	.409 \pm .006	.828 \pm .007
Latvian	Indo-European	Baltic	1,000	14.35	.387 \pm .005	.843 \pm .006
Ligurian	Indo-European	Romance	275	16.16	.495 \pm .011	.724 \pm .014
Lithuanian	Indo-European	Baltic	1,000	16.11	.338 \pm .005	.878 \pm .005
Livvi-Karelian	Uralic	Finnic	119	10.64	.401 \pm .017	.819 \pm .020
Low Saxon	Indo-European	Germanic	86	23.90	.440 \pm .012	.819 \pm .016
Maltese	Afro-Asiatic	Semitic	1,000	19.31	.368 \pm .004	.861 \pm .005
Manx	Indo-European	Celtic	1,000	7.78	.289 \pm .006	.860 \pm .007

Continued on next page

Table S1: (continued)

Language	Family	Group	N. Sents	Mean Sent. Length	$\langle H_{ks} \rangle \pm SE$	$\langle H_{deg} \rangle \pm SE$
Marathi	Indo-European	Indic	393	7.38	.412 \pm .015	.728 \pm .017
Mbyá Guaraní	Tupian	Maweti-Guarani	1,000	9.95	.447 \pm .006	.778 \pm .007
Moksha	Uralic	Mordvin	350	7.77	.390 \pm .012	.787 \pm .014
Mundurukú	Tupian	Mundurukú	113	6.81	.401 \pm .031	.735 \pm .032
Naija	<i>creole</i>		1,000	15.55	.601 \pm .006	.584 \pm .008
Nheengatu	Tupian	Maweti-Guarani	178	9.62	.422 \pm .016	.771 \pm .021
North Sami	Uralic	Sami	1,000	7.96	.533 \pm .010	.628 \pm .011
Norwegian	Indo-European	Germanic	1,000	15.06	.451 \pm .006	.774 \pm .008
Old Church Slavonic [†]	Indo-European	Slavic	1,000	10.14	.493 \pm .008	.719 \pm .009
Old E. Slavic [†]	Indo-European	Slavic	1,000	10.02	.453 \pm .008	.751 \pm .009
Old French [†]	Indo-European	Romance	1,000	10.39	.473 \pm .007	.718 \pm .009
Persian	Indo-European	Iranian	1,000	16.61	.386 \pm .004	.867 \pm .004
Polish	Indo-European	Slavic	1,000	10.80	.391 \pm .007	.819 \pm .008
Pomak	Indo-European	Slavic	1,000	12.17	.499 \pm .007	.704 \pm .009
Portuguese	Indo-European	Romance	1,000	15.61	.405 \pm .005	.802 \pm .006
Romanian	Indo-European	Romance	1,000	19.14	.409 \pm .004	.843 \pm .005
Russian	Indo-European	Slavic	1,000	14.45	.360 \pm .005	.861 \pm .006
Sanskrit [†]	Indo-European	Indic	1,000	7.75	.447 \pm .009	.723 \pm .011
Scottish Gaelic	Indo-European	Celtic	1,000	17.28	.400 \pm .005	.854 \pm .006
Serbian	Indo-European	Slavic	1,000	19.15	.377 \pm .004	.872 \pm .004
Sinhala	Indo-European	Indic	100	7.80	.433 \pm .017	.768 \pm .022
Skolt Sami	Uralic	Sami	216	9.83	.490 \pm .015	.705 \pm .018
Slovak	Indo-European	Slavic	1,000	9.34	.420 \pm .007	.778 \pm .008
Slovenian	Indo-European	Slavic	1,000	16.91	.435 \pm .005	.805 \pm .006
S. Levantine Arabic	Afro-Asiatic	Semitic	84	7.19	.345 \pm .026	.788 \pm .034
Spanish	Indo-European	Romance	1,000	24.28	.369 \pm .003	.872 \pm .004
Swedish	Indo-European	Germanic	1,000	15.59	.430 \pm .005	.808 \pm .006
Swedish Sign Language	<i>sign language</i>		169	9.17	.483 \pm .019	.734 \pm .020
Swiss German	Indo-European	Germanic	100	12.66	.530 \pm .016	.696 \pm .023
Tagalog	Austronesian	Central Philippine	178	8.12	.337 \pm .018	.869 \pm .016
Tamil	Dravidian	Southern	877	11.24	.410 \pm .009	.782 \pm .010
Tatar	Turkic	N.W.	145	12.74	.336 \pm .012	.881 \pm .012
Telugu	Dravidian	S.-Central	665	4.87	.398 \pm .015	.689 \pm .016
Thai	Tai-Kadai	Tai	995	21.94	.380 \pm .003	.888 \pm .004

Continued on next page

Table S1: (continued)

Language	Family	Group	N. Sents	Mean Sent. Length	$\langle H_{ks} \rangle \pm SE$	$\langle H_{deg} \rangle \pm SE$
Tupinambá [†]	Tupian	Maweti-Guarani	429	7.22	.436 ± .013	.749 ± .015
Turkish	Turkic	S.W.	1,000	8.94	.326 ± .007	.834 ± .008
Turkish/German	<i>code switching</i>		1,000	15.20	.544 ± .005	.692 ± .007
Ukrainian	Indo-European	Slavic	1,000	14.92	.376 ± .005	.845 ± .006
Umbrian [†]	Indo-European	Italic	80	8.28	.346 ± .029	.879 ± .024
Upper Sorbian	Indo-European	Slavic	635	14.16	.383 ± .005	.849 ± .007
Urdu	Indo-European	Indic	1,000	23.30	.426 ± .003	.845 ± .004
Uyghur	Turkic	S.E.	1,000	9.80	.375 ± .007	.816 ± .007
Vietnamese	Austro-Asiatic	Viet-Muong	1,000	12.86	.405 ± .005	.838 ± .006
Welsh	Indo-European	Celtic	1,000	17.88	.371 ± .005	.848 ± .006
W. Armenian	Indo-European	Armenian	1,000	15.13	.405 ± .005	.849 ± .006
W. Sierra Puebla Nahuatl	Uto-Aztecan	Nahuan	793	10.00	.418 ± .008	.787 ± .009
Wolof	Niger-Congo	N. Atlantic	1,000	18.25	.408 ± .005	.834 ± .005
Xibe	Tungusic	Jurchenic	736	14.28	.360 ± .007	.841 ± .008
Yakut	Turkic	N.E.	237	4.71	.360 ± .026	.690 ± .027
Yoruba	Niger-Congo	Defoid	308	21.81	.420 ± .006	.844 ± .007
Yupik	Eskimo-Aleut	Eskimoan	284	7.69	.440 ± .011	.802 ± .014
Zaar	Afro-Asiatic	W. Chadic	581	9.92	.555 ± .010	.617 ± .013

Algorithm S1 Find the maximum value of h_{deg} for a given number of vertices N .

Require: $N > 1$

$t \leftarrow$ array of $N - 1$ ones

$Seen \leftarrow \{t\}$

$Stack \leftarrow \{t\}$

$best \leftarrow 0$

while $Stack \neq \emptyset$ **do**

$t \leftarrow \text{pop}(Stack)$

$L \leftarrow \text{length}(t)$

$hist \leftarrow$ array containing histogram of values in t

$hist[0] \leftarrow N - L$

$p \leftarrow hist / \sum hist$

$v \leftarrow - \sum_{p[i] \neq 0} p[i] \log_2 p[i]$

if $v \geq best$ **then**

$best \leftarrow v$

end if

if $L > 1$ **then**

for $i = 0$ to $L - 1$ **do**

for $j = i + 1$ to $L - 1$ **do**

$t_2 \leftarrow t$

$t_2[i] \leftarrow t_2[i] + t_2[j]$

 Remove $t_2[j]$ from t_2

sort(t_2)

if $t_2 \notin Seen$ **then**

$Stack \leftarrow Stack \cup \{t_2\}$

$Seen \leftarrow Seen \cup \{t_2\}$

end if

end for

end for

end if

end while

return $best$

Algorithm S2 Construct a random directed tree with N vertices sampled by non-linear preferential attachment with exponent α . Returns the set of directed edges in the tree.

Require: $N > 0, \alpha \geq 0$

$Edges \leftarrow \emptyset$

$Nodes \leftarrow$ Set with elements $\{0, 1, \dots, N - 1\}$

$K \leftarrow$ Array of N integers, with indices starting at 0.

$root \leftarrow$ random sample uniformly an element from $Nodes$

$Linked \leftarrow \{root\}$

$Nodes \leftarrow Nodes - \{root\}$

$K[root] \leftarrow 1$

while $Nodes \neq \emptyset$ **do**

$newnode \leftarrow$ random sample uniformly an element from $Nodes$

$source \leftarrow$ random sample an element i from $Linked$ with probability proportional to $K[i]^\alpha$

$Nodes \leftarrow Nodes - \{newnode\}$

$Linked \leftarrow Linked \cup \{newnode\}$

$K[newnode] \leftarrow 1$

$K[source] \leftarrow K[source] + 1$

$Edges \leftarrow Edges \cup \{(source, newnode)\}$

end while

return $Edges$
